Title

Effect of alkanethiol chain length on the oxidation resistance of self-assembled monolayer passivated Ge(100) surfaces.

Authors

Shane Garvey,[†‡] Barbara Maccioni,[‡] Andrew C. Serino,[ϕ] Justin D. Holmes,[†¥] Michael Nolan,[‡] Nerissa Draeger,[ϕ] and Brenda Long.[†]

Affiliations

[†]School of Chemistry, University College Cork, Cork, T12 YN60, Ireland.

[¥]AMBER Centre, Environmental Research Institute, University College Cork, Cork, T23 XE10, Ireland.

[‡]Tyndall National Institute, University College Cork, Cork, T12 R5CP, Ireland.

[ϕ]Lam Research Corp., Fremont, CA 94538, USA.

Corresponding author email & address: brenda.long@ucc.ie School of Chemistry, University College Cork, Cork, T12 YN60, Ireland

The use of self-assembled monolayers (SAMs) of heteroalkanes as passivation layers to protect against oxidation has been studied on a variety of materials. However, typically heteroalkanes with C8 and longer have been used, since the contributing van der Waals between the carbon chains is a significant stabilising force and the longer the chain the greater the force. The industry requirement for passivating semiconducting materials is that they remain oxide free for a queue time of 24 h. The remit of this study is to explore whether passivation using shorter chain alkanethiols, which would be beneficial for reducing carbon, will work to prevent re-oxidation over this time frame. A series of 1-alkanethiols, with chain lengths from C2 to C12 are used to create SAMs on Ge(100) and a study of the re-oxidation of the passivated Ge upon exposure to ambient conditions is undertaken in an effort to determine how chain length effects oxidation resistance of the passivated Ge. X-ray photoelectron spectroscopy is used, complimented by water contact angle measurements to show that the longer thiol molecules outperform their shorter-chain counterparts at inhibiting re-oxidation over

168 h of exposure to ambient. Nonetheless, Ge surfaces passivated by the short-chain thiols, down to C4, still display acceptable resistance to re-oxidation. Finally, a detailed summary of density functional theory simulations whereby the most stable SAM structures and coverages are explored.

Keywords

Germanium, Semiconductor, Passivation, Self-Assembled Monolayers, Oxidation resistance, Alkanethiols.

1. Introduction

Ge is predicted to be the channel material for CMOS (complementary metal oxide semiconductor) devices for two main reasons. Firstly, it has both higher electron and hole mobilities than Si (over 2 and 4 times, respectively) meaning increased performance and a reduction in power consumption [1]. Secondly, due to its similarity to Si, also being a Group IV element, it is easier to integrate into current CMOS processing lines than the other potential high-mobility channel material candidates (transition metal dichalcogenides, III-Vs). However, the native Ge oxide (consisting largely

of GeO_2) exhibits characteristics that make it undesirable from a device perspective. For example, unlike SiO_2, GeO_2 is water-soluble and thus the aqueous processing steps that are currently used in device manufacturing would cause oxide etching and regrowth upon exposure to air. Multiple cycles of this, which would be typical along the processing line, would cause loss of Ge, an issue which is critical when working with Ge nanostructures such as nanoribbons or pillars [2]. Also, the interface between Ge and its native oxide is not ideal with vacancies that trap charge carriers and hinder device performance [3]. Consequently, methods to replace the Ge oxide are of interest to those who wish to circumvent the aforementioned issues to work towards enabling the use of Ge as a channel material in future CMOS devices.

Specifically, in relation to forming self-assembled monolayers (SAMs) on Ge, a review of the literature shows that there are three main methods. Namely, using Grignard-chemistry [4, 5], alkanethiol passivation [6, 7] and through hydrogermylation [8]. Both the Grignard chemistry and hydrogermylation approach result in the creation of Ge-C bonds whereas the alkanethiol passivation route involves the formation of Ge-S bonds [2]. The vast majority of the literature on alkanethiol ($CH_3(CH_2)_{n-1}SH$) passivation of

Ge pertains to 1-dodecanethiol ($C_{12}H_{26}S$) [9-13]. That said, Han et al. have demonstrated that SAMs of both 1-octadecanethiolates ($C_{18}H_{37}S$) and 1-octanethiolates ($CH_3(CH_2)_7S$) can be formed when an oxide-free, H-terminated Ge(111) surface is reacted with a solution of the thiol molecules [14]. In this study, alkanethiol passivation of oxide-free Ge is conducted using a range of aliphatic thiol molecules with carbon chain lengths from C2 to C12 in an effort to discern what effect, if any, the length of the thiol chain has on the effectiveness of the SAM at inhibiting Ge oxidation over the course of 168 h.

In general, surface passivation studies, centred around the use of SAMs of heteroallyl alkanes or allylalkenes are focused on carbon chain lengths of C8 and longer. The reason for this is that van der Waals (vdW) interactions between the carbon chains have been recognized as a significant factor in the stabilization of the SAM. However, there are several reasons why minimizing the chain length would be beneficial from an industrial perspective; 1) SAMs comprised of shorter chain length thiols would be easier to remove if and when needed due to the reduced effect of the vdW interactions between adjacent thiols. 2) Shorter chain length thiols have

higher vapour pressures and therefore are easier to promote into the vapor necessary to achieve vapor-phase passivation. Such methods are necessary when working with nanostructures since the destructive capillary forces that are experienced during wet-chemical processing can be avoided. 3) Less heat is required to achieve vaporization of short chain thiols. Reducing the processing temperatures required to achieve passivation is advantageous since a low thermal budget allows the passivation process to be carried out further down the device fabrication line and previous processing steps are less likely to be affected.

For the purposes of this study, the authors chose to focus on the Ge(100) surface only. Crystal orientation is a significant factor to consider when conducting passivation studies since orientation at the surface dictates how the material reconstructs to minimize the number of dangling bonds. In the case of Ge(100), the surface reconstructs to form buckled dimers.[15] This surface is easily oxidized when exposed to the ambient, however the oxide film can be easily etched using halide acids and the resulting Ge(100) surface is reactive to alkanethiol passivation, as carried out by the authors. For

modelling the surface chemistry of SAMs we use the Cl-terminated unreconstructed Ge(100) surface as a reference.

Alkanethiol-SAMs have been shown to be effective at inhibiting oxide growth on Ge upon exposure to the ambient [11, 16]. The alkanethiol passivation of Ge is a two-step process; removal of native oxide followed by alkanethiol passivation. The native oxide can be removed using acid halides (HX, X = F, Cl, Br) [17-21]. Removing the oxide using HF yields a H-terminated surface which can be further functionalized by thiol molecules. However, the H-terminated surface itself does not offer prolonged oxidation resistance, in fact, the surface begins to re-oxidize within minutes [22]. Oxide removal using HCl or HBr results in a halide terminated surface. Cl-termination, while still being reactive toward thiols, oxidizes at a slower rate when compared to H-terminated Ge surfaces [17] and therefore allows for alkanethiol passivation with less risk of concurrent oxide growth. Also, in a lab setting HCl is safer to use than HF – industrially, this is not a significant concern since vapor HF etchers are commonly utilized.

The stability of thiol-passivated Ge surfaces is dependent on a number of factors. Thiol chain length is hypothesized to be a critical factor in the stability of the SAM since longer thiol chains maximize the vdW interactions between adjacent thiol molecules in the SAM. VdW interactions are weak interactions that occur between atoms that are in close proximity to each other. In the case of a thiol-SAM, the $–CH_2$ units in the backbones of adjacent thiol molecules interact with one another. Although this local interaction is weak in nature, the global effect of many thiols interacting can be considerable.

In an effort to elucidate the impact of the thiol chain length on the stability of a SAM on Ge and its oxidation resistance we present a detailed investigation of the preparation and properties of thiol-SAM functionalized Ge and a set of first principles density functional theory (DFT) calculations of model SAM-Ge systems.

2. Method & Materials

2.1 Preparation of SAMs on Ge surfaces

Passivation of the Ge was achieved using a range of aliphatic thiol molecules purchased from Sigma-Aldrich using a vapor-phase method previously outlined.[16] Specifically, 97% ethanethiol (ET, C2), 99% 1-butanethiol (BT, C4), 99% 1-hexanethiol (HT, C6), 98.5% 1-octanethiol (OT, C8) and 98% 1-dodecanethiol (DT, C12) were used. For comparison, a Cl-terminated Ge surface was prepared also simply by dipping in 20% HCl for 10 minutes to remove the native oxide followed by drying under a stream of N_2. Between measurements, the samples were stored in a temperature and humidity controlled environment (Vötsch temperature test chamber). To emulate ambient conditions, the relative humidity (RH) and temperature were set to 40% and 20°C, respectively. The authors have previously explored what effect ambient humidity has on Ge(100) surfaces passivated with aliphatic thiols [23]. Water contact angle (WCA) measurements were taken directly after the passivation procedures to ensure passivation of the Ge surfaces had been achieved. X-ray photoelectron spectroscopy (XPS) measurements were taken directly after the passivation reaction and after 24 and 168 h of exposure to the controlled ambient environment.

2.2 Characterization methods

2.2.1 WCA Analysis

An image of a 50 µL drop of deionized water that was deposited on to the Ge surface was taken such that the angle between the water, Ge surface and air could be measured. Increased hydrophobicity of the passivated Ge surfaces is used as an indirect indication that the passivation layer is present.

2.2.2 XPS

Spectra were acquired on an Oxford Applied Research Escabase XPS System equipped with a CLASS VM 100 mm mean radius hemispherical electron energy analyzer with multichannel detectors in an analysis chamber with a base pressure of 5.0×10^{-7} Pa. A step size of 0.7 eV, pass energy of 50 eV and a dwell of 0.3 s was used for survey spectra which were swept twice. All core level scans other than the S 2p were acquired with a step size of 0.1 eV, a dwell time of 0.1 s and a pass energy of 20 eV averaged over 10 scans. The S 2p scans were acquired with a step size of 0.1 eV, a dwell time of 0.1 eV and a pass energy of 50 eV averaged over 20 scans in an effort to maximize the intensity of the S 2p peaks. A non-monochromated Al-Kα X-ray source (1486.58 eV) at 100 W power (10 mA, 10kV) was used for all scans. All

spectra were acquired at a take-off angle of 90° with respect to the analyzer axis and were charge corrected with respect to the C 1s photoelectric line at 284.8 eV. A Shirley type background was used for construction and peak fitting of synthetic peaks. Synthetic peaks were a mix of Gaussian-Lorenzian, the Ge 2p spectra were fit using Gaussian-Lorentzian peak shape GL(90) for the elemental Ge peak and Lorentzian peak shape LA(1.53,243) for all other peaks. The relative sensitivity factors used are from a CasaXPS library containing Scofield cross-sections. Oxide thickness was calculated using the method outlined previously by Murakami et al [24].

$$d_{GeO_2} = \lambda_{GeO_2} sin\theta \; ln\left(\frac{I_{Ge}^{\infty}}{I_{GeO_2}^{\infty}}\frac{I_{GeO_2}}{I_{Ge}} + 1\right)$$

Where λ_{GeO_2} is the inelastic mean free path for the Ge 2p transition, which is 0.9 nm; the photoemission angle θ is 90°; $I_{Ge}^{\infty}/I_{GeO_2}^{\infty}$ is the ratio of the Ge 2p signal from infinitely thick Ge to infinitely thick GeO_2 and is 1.73; I_{GeO_2} is the intensity of the of native oxide (GeO_2) peak from curve fitting the

Ge 2p feature; I_{Ge} is the intensity of the metallic Ge peak from curve fitting the Ge 2p transition.

2.3 First Principles Simulation Methodology

We studied alkanethiolate SAMs on the Ge(100) surface from first principles DFT using a basis set of periodic plane waves as implemented in the Vienna Ab Initio Software Package (VASP5.4) [25, 26]. The core electrons are described by projector augmented wave (PAW) [27] potentials and the exchange and correlation energies are approximated by the generalized gradient approximation (GGA) with the Perdew-Burke-Ernzerhof (PBE) [28] gradient corrected functional. In order to take into account the van der Waals interactions between alkanethiols, we used the DFT-D3 dispersion correction method [29] that incorporates the long-range dispersion contribution to the exchange-correlation PBE functional. We use the following valance electron configurations; for germanium; Ge $4s^2$ and $4p^2$, for chlorine; Cl $3s^2$ and $3p^5$, for sulfur; S $3s^2$ and $3p^4$ and for carbon; C$2s^2$ and $2p^4$. All the calculations use an energy cut-off for the valence electron

plane wave basis set of 420 eV and the convergence criteria for electronic relaxations and ionic relaxations are 10^{-4} eV and 0.02 eV/Å, respectively. In addition, the conjugate-gradient algorithm was used for the relaxation of the ions during the calculations, and a 2×2×1 Monkhorst–Pack k-points grid [30] was used for the integrals in the Brillouin zone for a correct energy convergence.

3. Results & Discussion

WCA analysis was conducted to give an insight into the wettability of the Ge surfaces directly after passivation. Alkanethiols, used in this study are terminated with $–CH_3$ groups, which water does not interact favourably with. Trends have been observed whereby SAMs consisting of C8 and C12 alkanethiols produce surfaces that are more hydrophobic than those passivated by shorter chain alkanethiols (C2, C4 and C6) [31]. This trend was generally observed, as can be seen by **Figure 1,** whereby hydrophobicity of the passivated Ge surfaces trends with the length of the thiol molecules used to achieve that passivation. SAMs produced using ET and BT yield Ge surfaces with approximately the same level of hydrophobicity however, as

the chains lengthen, the hydrophobicity of the surface increases to 100° for both OT- and DT-passivated Ge.

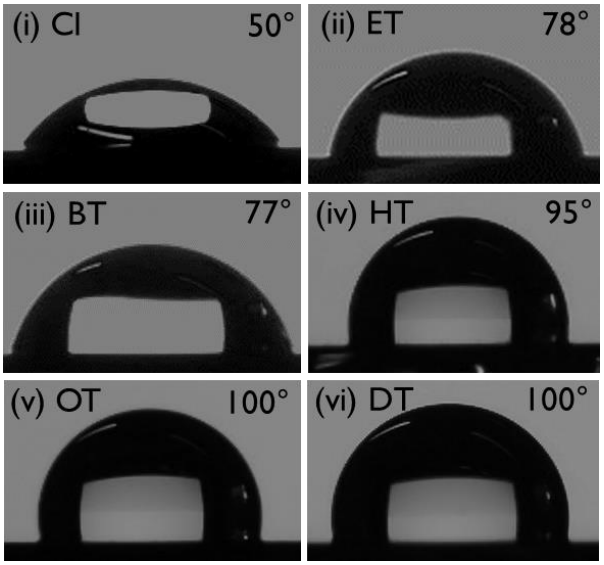

Figure 1. WCA analysis of Ge passivated by **(i)** Cl **(ii)** ET **(iii)** BT **(iv)** HT **(v)** OT and **(vi)** DT revealing what effect surface termination has on Ge hydrophobicity.

XPS is a standard method for probing SAMs since it allows for the elemental composition, chemical state and electronic structure of the surface of a material to be ascertained. It is used in this study to track the reoxidation of the passivated Ge(100) surfaces upon exposure to ambient conditions to

elucidate what effect thiol chain-length has on the effectiveness of the SAMs at inhibiting Ge oxidation. Thiol-SAMs have previously been shown to be effective at inhibiting oxidation of Ge [11]. It is hypothesized that the longer carbon chain is the better at preventing Ge oxidation since the SAM is stabilised by vdW forces between the C backbones of the adjacent thiol molecules. The global vdW interaction increases with thiol chain length and therefore the effectiveness of the passivation. What the authors would like to ascertain is how short the carbon chain can be to give sufficient oxidation resistance (*i.e* queue time of 24 h). Five thiol molecules (ET, BT, HT, OT, DT) were chosen for this study, each containing an even number of $–CH_2$ units in the thiol backbone. These molecules were used to passivate Ge and a study of the reoxidation of Ge upon exposure to ambient conditions was carried out.

The calculated GeO_2 thicknesses at the 0, 24 and 168 h measurements are graphically represented in **Figure 2** and tabulated in **Table 1**. For reference, a Cl-terminated Ge surface is included in the study as a baseline for Ge reoxidation upon exposure to ambient conditions. In the case of BT, HT, OT and DT no GeO_2 was detectable by XPS directly after passivation

(*i.e.* 0 h). This was not the case with ET-passivated Ge, whereby a non-negligible amount of Ge oxide (0.06 nm) is present after the passivation procedure. It is hypothesized that the alkanethiol chain is too short in the case of ET and so the SAM is not stabilised by the vdW forces between the adjacent C backbones. Consequently, the sample begins to oxidize in the short space of time (~ 5 minutes) that is required to clean the sample after passivation and to load into the XPS chamber.

From **Figure 2**, a clear pattern is observed whereby Ge oxidation trends with thiol chain length. That is, SAMs of thiol molecules consisting of longer chains inhibit the oxidation of Ge more effectively than SAMs comprised of shorter chains upon exposure to ambient conditions for 168 h. Over the course of the 168 h period, 0.08 nm of GeO_2 grows on the DT-passivated Ge whereas 0.12 nm and 0.14 nm and 0.16 nm grows on OT-, HT- and BT-passivated Ge, respectively. These results are tabulated in **Table 1** as well as the calculated oxide thicknesses for as-received Ge and Cl-terminated Ge with 0, 24 and 168 h of exposure to ambient conditions.

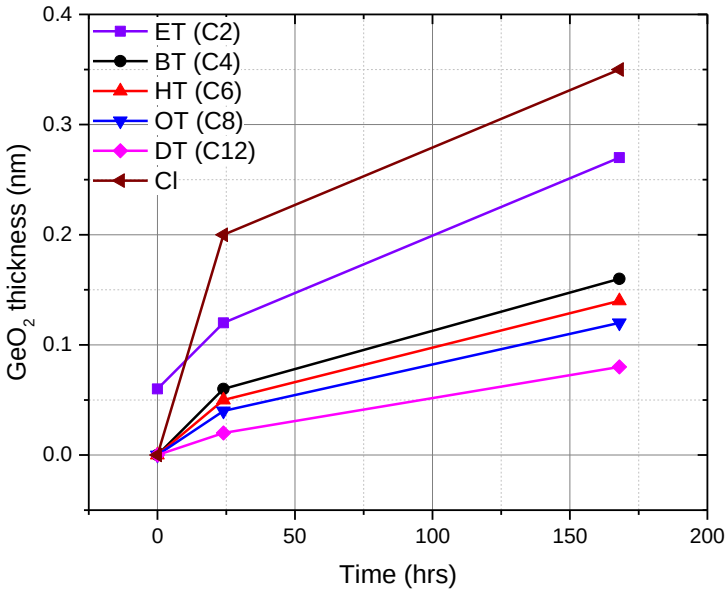

Figure 2. GeO_2 growth over 24 and 168 h for Ge passivated by ET (purple), BT (black), HT (red), OT (blue), DT (pink), Cl (brown).

Surface termination	As-Rec	Cl-Ge	ET (C2)	BT (C4)	HT (C6)	OT (C8)	DT (C12)
Exposure time (hrs)	Oxide Thickness (nm)						
0	2.12	0	0.06	0	0	0	0
24	2.12	0.2	0.12	0.06	0.05	0.04	0.02

168	2.12	0.35	0.27	0.16	0.14	0.12	0.08

Table 1. Calculated oxide thicknesses for Ge with a range of surface terminations.

In all cases, the rate of oxidation in the first 24 h is greater than the 144 h that follows indicating that the oxidation process slows in time likely as a saturation point is reached whereby the oxide layer terminates the Ge surface.

Sulfur acts as a useful marker when tracking the presence of thiol-SAMs on Ge by XPS. In **Figure 3 (i)**, the S 2p peaks for Ge passivated by the thiol molecules (C4, C6, C8, C12) with 0 h exposure to ambient conditions are shown and compared with freshly cleaned, as-received Ge (green). Again, ET-passivated Ge is omitted since GeO_2 is present at the 0 h measurement and so a comparison of oxidation resistance over 168 h is futile. In the case of the as-received Ge, as expected, there is no S peak present at 162.4 eV in **Figure 3 (i)** (green). There is however, a peak of approximately the same intensity present at 162.4 eV for the four passivated samples. Since each thiol molecule contains only one S atom, irrespective of the number of

C atoms present in the backbone of the thiol, a comparable amount of S on the surface indicates that the concentration of the thiol molecules on the Ge surface is similar in all cases. Thus, it can be inferred that the length of the thiol molecule does not have a considerable effect on the level of passivation achieved using the vapor-phase method outlined in the methods section. In **Figure 3 (ii)**, the C 1s peaks are presented for the same sample set. Here, the intensity of the C peak diminishes as the length of the thiol molecule decreases from 12 C to 4 C atoms. In contrast to S, the number of C atoms in each thiol molecule reduces by two from 1-dodecanethiol, with 12 C atoms through to 1-butanethiol with 4 C atoms, which explains the diminishing nature of the C peak from one sample to the next. Although the as-received Ge sample has been cleaned by sonication, C is detectable on the surface – as can be seen by the presence of the C 1s peak at 284.8 eV (green) in **Figure 3 (ii)**. The presence of C is due to contamination by adventitious C from the ambient prior to loading into the XPS instrument. This C peak is always present and is used to charge-correct the spectra that are acquired.

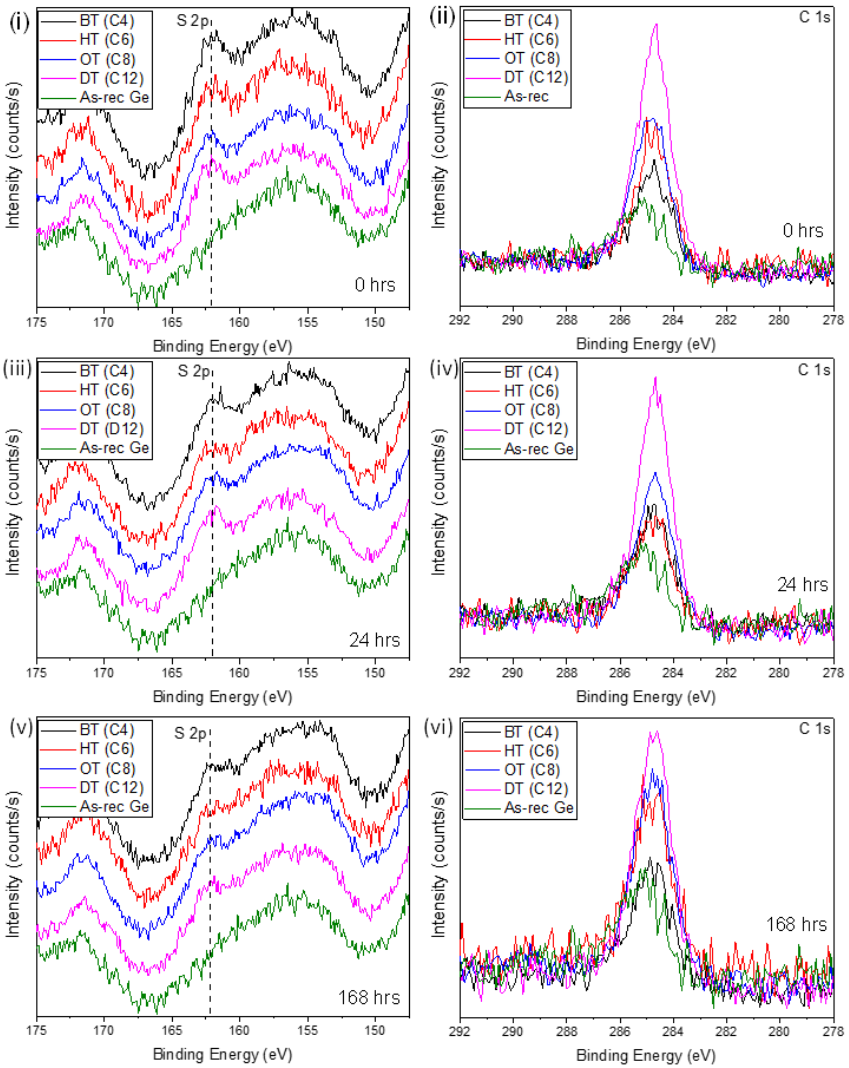

Figure 3. S 2p and C 1s spectra for as-received Ge and Ge passivated by BT (black), HT (red), OT (blue) and DT (pink) respectively with **(i) & (ii)** 0 h

(iii) & (iv) 24 h and **(v) & (vi)** 168 h exposure to the ambient. S 2p spectra are linearly offset along the y-axis for the purpose of comparison. C 1s spectra are overlaid with no offset.

Having exposed the sample set to the ambient for a period of 24 h, XPS measurements were taken again. The S 2p and C 1s data are displayed in **Figure 3 (iii) & (iv)**. By tracking the changes in intensity of the S 2p and C 1s peaks along with calculated GeO_2 thicknesses (**Figure 2**), the authors can determine how well each passivating SAM prevents oxidation of the Ge. Again, in all cases, there is an S 2p peak present at 162.4 eV; however, the amount of S has diminished somewhat from the first measurement taken directly after the passivation procedure. The diminishing S 2p signal is likely due to the growth of Ge oxide evidenced by the slight increase in the calculated GeO_2 thickness in **Figure 2**.

In **Figure 3 (v) & (vi)**, a continuation of the trend that has been observed from 0 to 24 h is evident. After 168 h of exposure to the ambient conditions, an S signal is still observed for the passivated samples albeit at lower intensity than at the 0 and 24 h measurements. A comparison of the S

2p signals for each sample is displayed in **Figure 6**. In all cases, there is a drop in the intensity of the S signal over 168 h. The diminishing nature of the S 2p peak over the course of 168 h of exposure to ambient conditions can be understood when the growth of the native oxide (**Figure 2)** is considered also. Ge-S bonds are replaced by Ge-O bonds resulting in the appearance of peaks relating to Ge^{+2} (GeO) and Ge^{+4} (GeO_2) in the Ge 2p XPS spectra resulting in thicker calculated oxide thicknesses (**Table 1**) and the reduced intensity of the S 2p peaks.

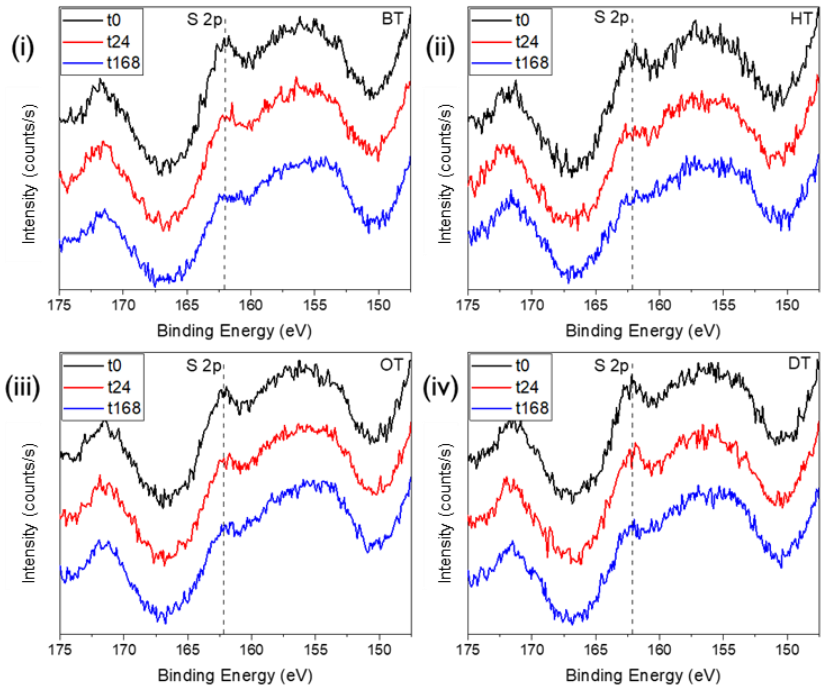

Figure 4. Overlaid S 2p spectra for Ge passivated by **(i)** BT **(ii)** HT **(iii)** OT and **(iv)** DT after 0 (black), 24 (red) and 168 (blue) h of exposure to the ambient. Spectra are linearly offset along the y-axis for the purpose of comparison.

Generally, there is a drop in intensity of the C 1s peak from 0 (black) to 24 (red) to 168 (blue) h as illustrated in **Figure 5**. However, since contamination from the ambient is likely to affect the C data, it is best to

follow the S 2p trends, as S is specific to the thiol molecules. With that said, a general trend whereby C concentration on the Ge surface decreases over 168 h is observed. This indicates that over 168 h of exposure to ambient conditions, thiol desorption from the Ge surface occurs in all cases, irrespective of thiol chain length.

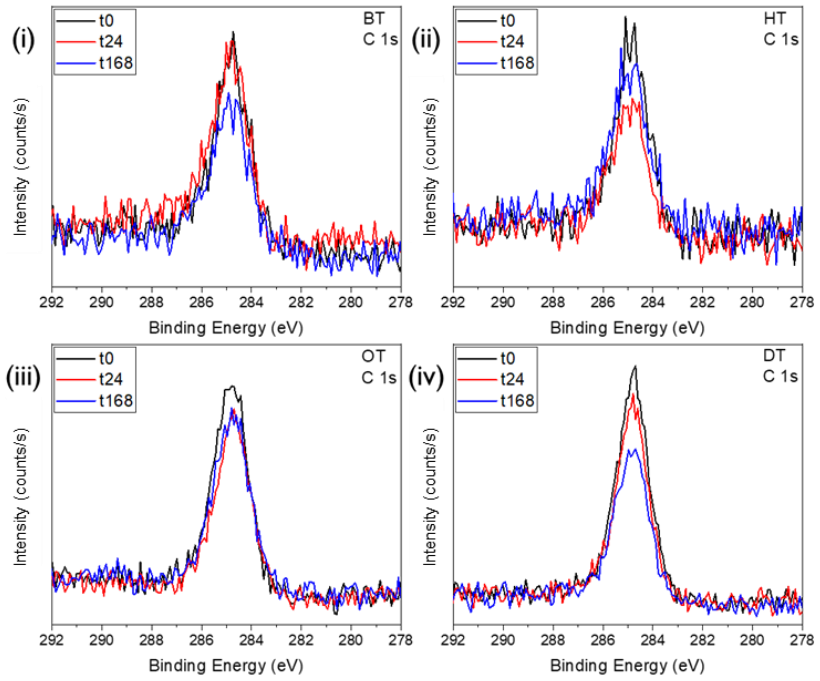

Figure 5. C 1s spectra for Ge passivated by **(i)** BT **(ii)** HT **(iii)** OT and **(iv)** DT after 0 (black), 24 (red) and 168 (blue) h exposure to the ambient. Spectra are overlaid with no y-axis offset.

DFT calculations were performed to understand the atomic level details of the role of length of the thiol molecule on the stability of thiol-SAM passivated Ge(100) surfaces. The Ge(100) surface is modelled with a (2x2) surface supercell expansion with 128 atoms. To simulate the conditions of

the bulk, Ge atoms in the bottom layer of the slab are fixed. The top surface, composed by 8 Ge atoms, was initially fully passivated with Cl atoms. Surface calculations were performed using the slab technique, taking into account the periodically repeating infinite layers separated by vacuum layers along the normal surface. A vacuum thickness of 40 Å is adopted in all cases in order to remove interaction between periodic slabs perpendicular to the surface, while allowing for a range of alkanethiol chain lengths from 4 to 12 C atoms to be explored.

To determine the stable structures and coverages, we calculated the adsorption energy of alkanethiols on the Ge(100) surface for different thiols with an even number of C atoms in the molecule backbone and at various coverages. Coverages from 12.5% to 100% can be constructed in our Ge surface model. We considered the adsorption of the thiols in thiolated form since it is well established that the S–H bond breaks during the adsorption of thiols on germanium surfaces leading to HCl elimination and Ge-S bonding. The adsorption energies (E_{ads}) of the thiols forming the SAMs were computed by the following expression:

$$E_{ad} = E(tot) + E(n\ HCl) - [\ E\ (Cl{:}Ge) + E(\ n\ HS\text{-}C_xH_{2x+1})\ ]$$ **(eqn. 1)**

where E(tot) is the total energy of the thiol-functionalized Ge surface, with *n* adsorbed thiol molecules; E(*n* HCl) is the energy of the isolated HCl molecule multiplied by the number, *n*, of HCl molecules; E (Cl:Ge) is the energy of the Cl passivated Ge(100) surface and E (nHS-C_xH_{2x+1}) is the energy of *n* alkanethiol molecules. All the energies have been computed using the same parameters including the vdW corrections. Negative values of the adsorption energies E_{ads} mean energetically favored adsorption configurations.

The most stable configurations for the thiol-SAMs were determined, starting from several initial trial configurations and adsorption sites on the Ge(100) surface, by energy minimizations to sample minima corresponding to equilibrium structures. The results for the computed adsorption energies of Ge(100) passivated by thiols with an even number of $–CH_2$ units in the chains (C4, C6, C8, C12) are reported in **Figure 6**.

Surface passivation of Ge(100) is favorable for all thiols for coverages above 37.5%. In general, we find that coverages between 75% and

100% are the most favorable, except for the BT (C4) where it is 62.5%, although the higher coverages are still favorable (negative adsorption energy from **eqn. 1**). Referring to the computed adsorption energies, the most strongly bound thiol is the HT (C6), although at the most stable coverages all thiols show high stability, with computed adsorption energies of between -2.0 and -4.5 eV/molecule, which indicates a strong thiol-surface bond. By contrast, in a previous study, on H:Si(111) we found weaker adsorption energies around -1.5 eV [32]. OT and DT (C8 and C10) show similar behavior while BT (C4) appears to show a stronger coverage dependence, with adsorption energies initially comparable with C8 and C10 thiols at low coverage, but being less favorable at high coverages.

These results are comparable to experimental data, in which the Ge passivation with thiols from butanethiol to dodecanethiol are favorable, while the precise coverage does not have a strong an impact on stability.

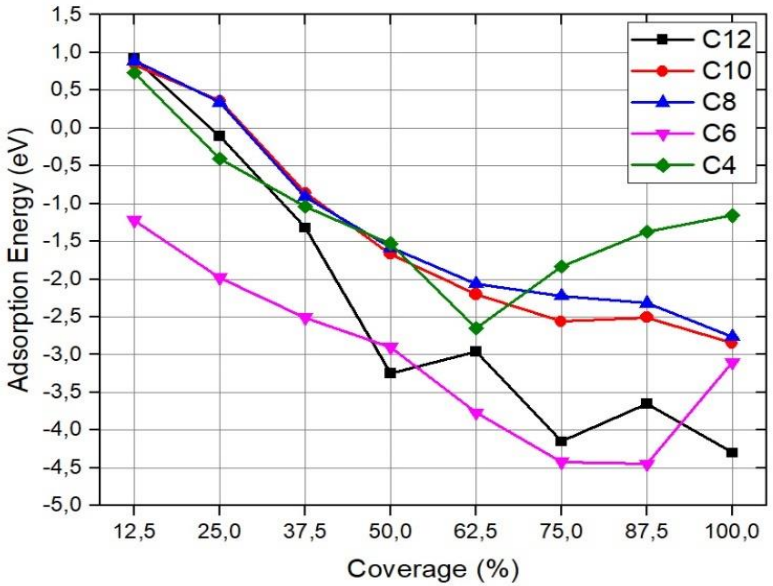

Figure 6. Adsorption energies of Ge(100) passivated by thiols at different lengths as a function of the coverage.

In order to understand the E_{ads} values, we have analyzed the structural properties of the Ge-SAM systems. We began our investigation by determining the most favorable configurations for the Ge(100) passivation in which chlorine and sulfur atoms occupy the same Cl–Ge–Cl and S–Ge–S bridge sites [33, 34]. The interatomic distances for the Ge–Cl and Ge–S

bonds are 2.4 Å and the distance between Ge atoms is 4.1 Å in both chlorine- and sulfur- passivated Ge(100).

The binding of the alkanethiols induces significant distortions to the surface upon relaxation whereby S atoms move towards the bridge site. In the most favorable configurations, the interatomic distances for the Ge–S bonds in butane- and hexane-thiolates on Ge(100) are between 2.2 Å and 2.4 Å and thus vary at most by 0.2 Å. The interatomic distances for the Ge–S bonds in the longer chains, i.e. C8, C10 and C12, are between 2.2 Å and 2.6 Å, varying at most by 0.4 Å. This variation is more evident in configurations at coverages between 75% and 100%, in which some S atoms bond to only one Ge surface atom.

The corresponding S–C distances for all thiolates at all coverages, vary by only 0.02 Å between 1.82 Å and 1.84 Å. At lower coverages, from 12.5% to 37%, the S–C distance is constant across all the thiol chains and assumes a maximum value of 1.84 Å. As the coverage increases, the S–C distance for the thiols assumes different values. Consequently, the interatomic distances within the molecule do not depend significantly on the

length of the thiolate chains, but depend on the particular arrangement of thiols on the Ge surface.

Moreover, from structural analysis, we have found that the alkanethiols form a compact monolayer with a non-homogeneous thickness. The thiol chain thickness can be determined as the projection of the length of the chain along the c-axis, denoted by l_c in **Figure 7**. We have computed the thickness for every alkanethiol-SAM with 4, 6, 8, 10 and 12 carbon atoms that entirely cover the Ge surface and at the relevant, most stable partial coverages. The difference in the thickness is related to the simultaneous variation of the length and the tilt angle, l and θ, respectively, of each chain forming the monolayer. The tilt angle, defined in **Figure 7**, corresponds to the angle between the thiol chain and the normal to the surface at the adsorption point. The angles are measured between the c-axis and the straight line joining S and C_n (n = 4, 6, 8, 10, 12). On gold [35, 36], and silicon [37] surfaces, thiols usually adopt a tilted structure which can promote interactions between the chains and consequent stabilization of the system.

The arrangement of SAMs on top of the Ge surface also exhibit a precession angle (α), which is used to demonstrate the coexistence of

differently oriented chains. The precession angle (α) corresponds to the angle between thiol chain projection into the ab plane (surface) and the a-axis (**Figure 7**) [38].

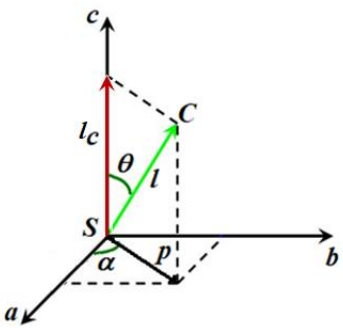

Figure 7. Definition of the tilt angle (θ), precession angle (α), thiol chain length (l), thiol chain thickness (l_c) and thiol chain projection (p) in ab-plane. S denotes the sulfur atom and C denotes the carbon atom at the end of the thiol chain. In particular, the tilt and the precession angles are measured between the c-axis and the line joining S and carbon C; and between the a-axis and the projection line, respectively.

The tilt of the chains is more pronounced in the case of short-chain thiol-passivated Ge (C4 and C6). Furthermore, an increase of the tilt angles

in C4 chains up to 35° is found at low coverages; at full coverage, this angle assumes the minimum value of 4°. The precession angles obtained indicate different chain orientation at low coverage. At the most stable coverage and at full coverage, average precession angles of 180° and 220° (for C4 and C6, respectively) indicate that the thiol chains are well ordered. This ordering in the thiol-SAM structure is one origin of enhanced stability at higher coverages where the ordering promotes the interchain vdW interactions.

The tilt angle in OT (C8) chains assumes a maximum value of 36° between coverages of 37.5% and 75% and this angle decreases to 2° at higher coverages. In addition, the precession angle increases from 154° to 230° as the coverage increases from 75% to 100%. In this case, the chains are oriented in two different directions, with precession angles of 205° and 230°, and assume two values of tilt angle; 9° and 3°, respectively. Long-chain thiols at stable coverages adopt two different directions. We find precession angles of 88° - 226° for C10, and 80° - 226° for C12, while the tilt angles are 4° - 14° and 4° - 12° respectively.

In **Figure 8,** we present two different views of the most favorable configurations for these thiols. Short-chain thiols tend to assume one orientation while long-chain thiols tend to be more ordered on the surface and assume two orientations. The roles of chain length, angles and coverage on the adsorption characteristics have been examined to elucidate the energetics of the Ge-SAM systems. The difference in energies and especially tilt angles indicates that alkanethiolates with long chains promote the stability of the SAM.

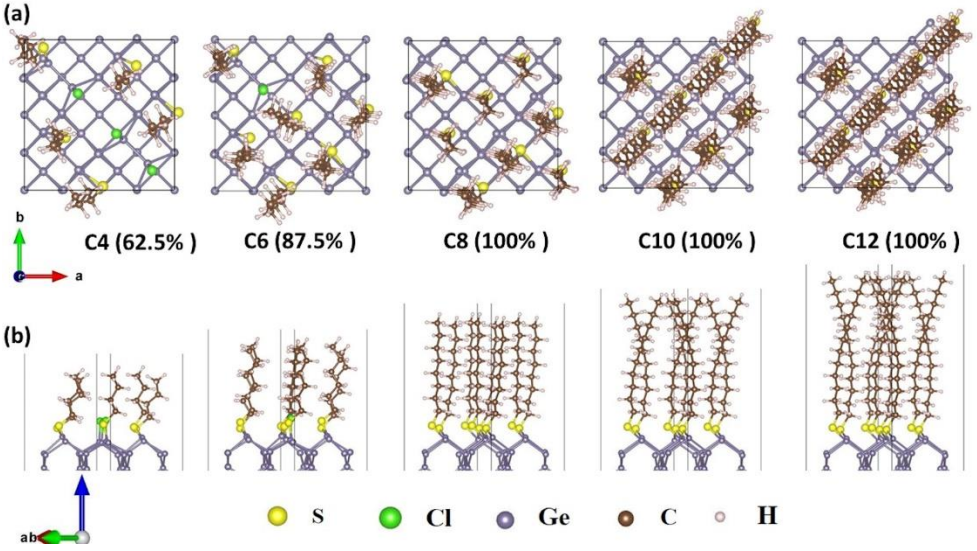

Figure 8. Top **(a)** and side **(b)** views of geometrically optimized structures of the most stable coverage for each thiol molecule.

4. Conclusions

The data has shown that resistance to oxidation of thiol-passivated Ge(100) is dependent on the length of the thiol chain. Longer chain thiols with an even number of $–CH_2$ units in their backbones outperform their shorter-chain counterparts. Calculated adsorption energies confirm that passivation of Ge(100) is more favorable when the number of carbon atoms in the thiol molecule is increased, although even Ge passivated by the short-chain BT-SAM exhibits acceptable resistance to reoxidation and therefore offers a passivation method that reduces C content on the Ge surface. Stability with coverage appears to be governed by the tilting and orientation of the thiolate chains on the Ge surface. The increased oxide resistance of Ge passivated by the longer-chain thiols is hypothesized to originate from the increased effect of the vdW interactions between adjacent thiol molecules in the SAM. The interaction between the thiol molecules stabilises the SAM, which acts as a

barrier between the Ge and air. The interaction between the shorter chain thiols in a SAM is less since there are fewer $–CH_2$ units per thiol. VdW interactions have been shown to play a central role in the stability of thiol-SAMs on gold [39] and here it is shown to be an important factor in the oxidation resistance of thiol-passivated Ge. Understanding Ge passivation methods are necessary if the complexities of the native oxide are to be avoided and Ge's potential as being the channel material in future logic devices is to be realized.

Author Contributions

The manuscript was written through contributions of all authors. All authors have given approval to the final version of the manuscript.

Funding Sources

The authors acknowledge financial support from Enterprise Ireland (EI IP 2018 0757A) and Lam Research Corporation and access to computing resources at Irish Centre for High End Computing (ICHEC).

5. References

[1] C. Claeys, E. Simoen, Introduction, in: Germanium-Based Technologies: From Materials to Devices. S. Claeys, E. Simoen, Eds., Elsevier Science, 2007, pp 1-10. https://doi.org/10.1016/B978-008044953-1/50004-1.
[2] P.W. Loscutoff, S.F. Bent, Reactivity of the Germanium Surface: Chemical Passivation and Functionalization, Annual Review of Physical Chemistry, 57 (2006) 467-495, DOI: https://doi.org/10.1146/annurev.physchem.56.092503.141307.
[3] J.R. Weber, A. Janotti, C.G. Van de Walle, Dangling Bonds and Vacancies in Germanium, Physical Review B, 87 (2013) 035203, DOI: https://doi.org/10.1103/PhysRevB.87.035203.
[4] G.W. Cullen, J.A. Amick, D. Gerlich, The Stabilization of Germanium Surfaces by Ethylation, Journal of The Electrochemical Society, 109 (1962) 124-127, DOI: https://doi.org/10.1149/1.2425342.

[5] J. He, Z.-H. Lu, S.A. Mitchell, D.D.M. Wayner, Self-Assembly of Alkyl Monolayers on Ge(111), Journal of the American Chemical Society, 120 (1998) 2660-2661, DOI: https://doi.org/10.1021/ja974119s.
[6] P. Ardalan, Y. Sun, P. Pianetta, C.B. Musgrave, S.F. Bent, Reaction Mechanism, Bonding, and Thermal Stability of 1-Alkanethiols Self-Assembled on Halogenated Ge Surfaces, Langmuir, 26 (2010) 8419-8429, DOI: https://doi.org/10.1021/la904864c.
[7] M.R. Kosuri, R. Cone, Q. Li, S.M. Han, B.C. Bunker, T.M. Mayer, Adsorption Kinetics of 1-Alkanethiols on Hydrogenated Ge(111), Langmuir, 20 (2004) 835-840, DOI: https://doi.org/10.1021/la035521p.
[8] K. Choi, J.M. Buriak, Hydrogermylation of Alkenes and Alkynes on Hydride-Terminated Ge(100) Surfaces, Langmuir, 16 (2000) 7737-7741, DOI: https://doi.org/10.1021/la000413d.
[9] Q. Cai, B. Xu, L. Ye, Z. Di, S. Huang, X. Du, J. Zhang, Q. Jin, J. Zhao, 1-Dodecanethiol Based Highly Stable Self-Assembled Monolayers for Germanium Passivation, Applied Surface Science, 353 (2015) 890-901, DOI: https://doi.org/10.1016/j.apsusc.2015.06.174.
[10] J.N. Hohman, M. Kim, H.R. Bednar, J.A. Lawrence, P.D. McClanahan, P.S. Weiss, Simple, Robust Molecular Self-Assembly on Germanium, Chemical Science, 2 (2011) 1334-1343, DOI: https://doi.org/10.1039/C1SC00115A.
[11] G. Collins, D. Aureau, J.D. Holmes, A. Etcheberry, C. O'Dwyer, Germanium Oxide Removal by Citric Acid and Thiol Passivation from Citric Acid-Terminated Ge(100), Langmuir, 30 (2014) 14123-14127, DOI: https://doi.org/10.1021/la503819z.
[12] G. Collins, P. Fleming, S. Barth, C. O'Dwyer, J.J. Boland, M.A. Morris, J.D. Holmes, Alkane and Alkanethiol Passivation of Halogenated Ge Nanowires, Chemistry of Materials, 22 (2010) 6370-6377, DOI: https://doi.org/10.1021/cm1023986.
[13] F.W. Yuan, H.J. Yang, H.Y. Tuan, Alkanethiol-Passivated Ge Nanowires as High-Performance Anode Materials for Lithium-Ion Batteries: The Role of Chemical Surface Functionalization, ACS Nano, 6 (2012) 9932-9942, DOI: https://doi.org/10.1021/nn303519g.
[14] S.M. Han, W.R. Ashurst, C. Carraro, R. Maboudian, Formation of Alkanethiol Monolayer on Ge(111), Journal of the American Chemical Society, 123 (2001) 2422-2425, DOI: https://doi.org/10.1021/ja993816c.

[15] H.J.W. Zandvliet, The Ge(001) Surface, Physics Reports, 388 (2003) 1-40, DOI: https://doi.org/10.1016/j.physrep.2003.09.001.
[16] S. Garvey, J.D. Holmes, Y.S. Kim, B. Long, Vapor-Phase Passivation of Chlorine-Terminated Ge(100) using Self-Assembled Monolayers of Hexanethiol, ACS Applied Materials & Interfaces, 12 (2020) 29899-29907, DOI: https://doi.org/10.1021/acsami.0c02548.
[17] J. Kim, J. McVittie, K. Saraswat, Y. Nishi, S. Liu, S. Tan, Germanium Surface Cleaning with Hydrochloric Acid, ECS Transactions, 3 (2006) 1191-1196, DOI: https://doi.org/10.1149/1.2355913.
[18] J.Y. Kim, J. McVittie, K. Saraswat, Y. Nishi, Passivation Studies of Germanium Surfaces, Solid State Phenomena, 134 (2008) 33-36, DOI: 10.4028/www.scientific.net/SSP.134.33.
[19] D.H. van Dorp, D. Weinberger, S. Van Wonterghem, S. Arnauts, K. Strubbe, F. Holsteyns, S. De Gendt, Nanoscale Etching: Dissolution of III-As and Ge in HCl/H2O2 Solutions, ECS Transactions, 69 (2015) 235-242, DOI: https://doi.org/10.1149/06908.0235ecst.
[20] K. Park, Y. Lee, J. Lee, S. Lim, Oxidation Mechanism of Hydrogen-Terminated Ge(100) Surface, Applied Surface Science, 254 (2008) 4828-4832, DOI: https://doi.org/10.1016/j.apsusc.2008.01.114.
[21] A. Molina, J.R. Shallenberger, S.E. Mohney, Vapor Phase Passivation of (100) Germanium Surfaces with HBr, Journal of Vacuum Science & Technology A, 38 (2020) 023208, DOI: https://doi.org/10.1116/1.5141941.
[22] D. Bodlaki, H. Yamamoto, D.H. Waldeck, E. Borguet, Ambient Stability of Chemically Passivated Germanium Interfaces, Surface Science, 543 (2003) 63-74, DOI: https://doi.org/10.1016/S0039-6028(03)00958-0.
[23] S. Garvey, A. Serino, M.B. Maccioni, J.D. Holmes, M. Nolan, N. Draeger, E. Gurer, B. Long, Towards Ge-based electronic devices: Increased longevity of alkanethiol-passivated Ge(100) in low humidity environments, Thin Solid Films, 759 (2022) 139466, DOI: https://doi.org/10.1016/j.tsf.2022.139466.
[24] H. Murakami, T. Fujioka, A. Ohta, T. Bando, S. Higashi, S. Miyazaki, Characterization of Interfaces between Chemically Cleaned or Thermally Oxidized Germanium and Metals, 33 (2010) 253, DOI: https://doi.org/10.1149/1.3487556.
[25] G. Kresse, J. Furthmüller, Efficiency of Ab-Initio Total Energy Calculations for Metals and Semiconductors using a Plane-Wave Basis Set,

Computational Materials Science, 6 (1996) 15-50, DOI: https://doi.org/10.1016/0927-0256(96)00008-0.
[26] G. Kresse, J. Furthmüller, Efficient Iterative Schemes for Ab-Initio Total-Energy Calculations using a Plane-Wave Basis Set, Physical Review B, 54 (1996) 11169-11186, DOI: https://doi.org/10.1103/PhysRevB.54.11169.
[27] P.E. Blöchl, Projector Augmented-Wave Method, Physical Review B, 50 (1994) 17953-17979, DOI: https://doi.org/10.1103/PhysRevB.50.17953.
[28] J.P. Perdew, K. Burke, M. Ernzerhof, Generalized Gradient Approximation Made Simple, Physical Review Letters, 77 (1996) 3865-3868, DOI: https://doi.org/10.1103/PhysRevLett.77.3865.
[29] S. Grimme, J. Antony, S. Ehrlich, H. Krieg, A Consistent and Accurate Ab-Initio Parametrization of Density Functional Dispersion Correction (DFT-D) for the 94 Elements H-Pu, The Journal of Chemical Physics, 132 (2010) 154104, DOI: https://doi.org/10.1063/1.3382344.
[30] H.J. Monkhorst, J.D. Pack, Special Points for Brillouin-Zone Integrations, Physical Review B, 13 (1976) 5188-5192, DOI: https://doi.org/10.1103/PhysRevB.13.5188.
[31] F. Ben Amara, E.R. Dionne, S. Kassir, C. Pellerin, A. Badia, Molecular Origin of the Odd–Even Effect of Macroscopic Properties of n-Alkanethiolate Self-Assembled Monolayers: Bulk or Interface?, Journal of the American Chemical Society, 142 (2020) 13051-13061, DOI: https://doi.org/10.1021/jacs.0c04288.
[32] H.H. Arefi, M. Nolan, G. Fagas, Density Functional Theory with van der Waals Corrections Study of the Adsorption of Alkyl, Alkylthiol, Alkoxyl, and Amino-Alkyl Chains on the H:Si(111) Surface, Langmuir, 30 (2014) 13255-13265, DOI: https://doi.org/10.1021/la502488c.
[33] T. Hayashi, Y. Morikawa, H. Nozoye, Adsorption State of Dimethyl Disulfide on Au(111): Evidence for Adsorption as Thiolate at the Bridge Site, The Journal of Chemical Physics, 114 (2001) 7615-7621, DOI: https://doi.org/10.1063/1.1360245.
[34] M.C. Vargas, P. Giannozzi, A. Selloni, G. Scoles, Coverage-Dependent Adsorption of CH3S and (CH3S)2 on Au(111): a Density Functional Theory Study, The Journal of Physical Chemistry B, 105 (2001) 9509-9513, DOI: https://doi.org/10.1021/jp012241e.

[35] L. Ramin, A. Jabbarzadeh, Odd–Even Effects on the Structure, Stability, and Phase Transition of Alkanethiol Self-Assembled Monolayers, Langmuir, 27 (2011) 9748-9759, DOI: https://doi.org/10.1021/la201467b.
[36] J.L.C. Fajín, F. Teixeira, J.R.B. Gomes, M.N.D.S. Cordeiro, Effect of van der Waals Interactions in the DFT Description of Self-Assembled Monolayers of Thiols on Gold, 9th Congress on Electronic Structure: Principles and Applications (ESPA 2014): A Conference Selection from Theoretical Chemistry Accounts, (2016) 127-139, DOI: https://doi.org/10.1007/978-3-662-49221-5_14.
[37] J.M. Castillo, M. Klos, K. Jacobs, M. Horsch, H. Hasse, Characterization of Alkylsilane Self-Assembled Monolayers by Molecular Simulation, Langmuir, 31 (2015) 2630-2638, DOI: https://doi.org/10.1021/la504178g.
[38] B. Szefczyk, R. Franco, J.A.N.F. Gomes, M.N.D.S. Cordeiro, Structure of the Interface Between Water and Self-Assembled Monolayers of Neutral, Anionic and Cationic Alkanethiols, Journal of Molecular Structure: Theochem, 946 (2010) 83-87, DOI: https://doi.org/10.1016/j.theochem.2009.11.021.
[39] M.S. Inkpen, Z.F. Liu, H. Li, L.M. Campos, J.B. Neaton, L. Venkataraman, Non-Chemisorbed Gold–Sulfur Binding Prevails in Self-Assembled Monolayers, Nature Chemistry, 11 (2019) 351-358, DOI: https://doi.org/10.1038/s41557-019-0216-y.